frontiers in Earth Science

ORIGINAL RESEARCH
published: 11 February 2022
doi: 10.3389/feart.2022.821305

Experimental Study on Thermal Regime and Frost Jacking of Pile Foundation During Operation Period in Permafrost Regions

Yunhu Shang[1,2], *Fujun Niu*[1]*, *Jianhong Fang*[3] *and Libo Wu*[4]

[1]*State Key Laboratory of Frozen Soil Engineering, Northwest Institute of Eco-Environment and Resources, Chinese Academy of Sciences, Lanzhou, China,* [2]*Da Xing'anling Observation and Research Station of Frozen-Ground Engineering and Environment, Northwest Institute of Eco-Environment and Resources, Chinese Academy of Sciences, Jiagedaqi, China,* [3]*Qinghai Research Institute of Transportation, Xining, China,* [4]*School of Civil Engineering and Hydraulic Engineering, Ningxia University, Yinchuan, China*

OPEN ACCESS

Edited by:
Guo Donglin, Institute of Atmospheric Physics (CAS), China

Reviewed by:
Yao Xiao, Northwest Institute of Eco-Environment and Resources (CAS), China
Yinghong Qin, Guangxi University for Nationalities, China

***Correspondence:**
Fujun Niu
niufujun@lzb.ac.cn

Specialty section:
This article was submitted to Cryospheric Sciences, a section of the journal Frontiers in Earth Science

Received: *24 November 2021*
Accepted: *13 January 2022*
Published: *11 February 2022*

Citation:
Shang Y, Niu F, Fang J and Wu L (2022) Experimental Study on Thermal Regime and Frost Jacking of Pile Foundation During Operation Period in Permafrost Regions. Front. Earth Sci. 10:821305. doi: 10.3389/feart.2022.821305

The stability of a cast-in-place pile foundation in permafrost region is primarily subject to the thermal regime and tangential frost-heave forces (TFF) during the operation period. However, studies focusing on the thermal and mechanical characteristics of pile foundation during runtime are rare. To investigate the effect of pile foundation on the thermal regime and quantify the magnitude of unit tangential frost-heave forces (UTFF), a field experiment was conducted on the Qinghai–Tibet Plateau, China. Results showed that the cast-in-place pile foundation enhanced the heat exchange between the atmosphere and soil, which expanded the annual range of the surrounding ground temperature. Furthermore, the permafrost table depth was increased by 0.4–0.7 m (0.33–0.58 times the pile diameter). The TFF increased significantly when the soil temperature decreased from 0 to −0.5°C. Meanwhile, the thickness of the frost heaving layer was approximately double that of the active layer, in which the maximum UTFF was higher than 52.04 kPa. The adfreezing bond force of permafrost to pile shaft burdened most of the applied load, and the end bearing contributed relatively little. Findings from this study will benefit the stability maintenance and structure design of pile foundation in permafrost regions.

Keywords: tangential frost-heave forces, cast-in-place pile foundation, thermal regime, permafrost region, frost heaving, frost jacking

INTRODUCTION

The cast-in-place pile foundation was first widely adopted in Qinghai–Tibet Plateau permafrost regions. Owing to its superior mechanical stability, more cast-in-place pile foundations will be constructed under the scenarios of the promotion of road grading. More than 80% of the bearing capacity of pile foundation in permafrost regions, irrespective of their types, is provided by adfreezing force between the surrounding frozen soil and the pile shaft (Aksenov and Kistanov, 2008). Adfreezing force is highly sensitive to temperature changes (Goncharov, 1965; Wang et al., 2005; Ma and Wang, 2014); hence, the thermal regime can affect the safety of pile foundation. To understand the stability of pile foundation more effectively during operation in permafrost regions, the interactive thermal effect between the pile foundation and the permafrost environment must be discussed. For the thermal regime of the cast-in-place pile foundation in permafrost, previous studies have primarily focused on the disturbance of hydration (Jia et al., 2004; Wu et al., 2006; Tang and Yang, 2010), temperature optimization of casting concrete (Wu et al., 2004; Li et al., 2005), and freeze-back time (Wang et al., 2004; Wang et al., 2005; Yuan et al., 2005; Zhang et al., 2010; Wang et al., 2013). Although these studies have emphasized on the thermal characteristics of pile foundation in the construction period, analyses of the thermal regime during the operation period are lacking.

In addition to the thermal regime, the seasonal frost heaving of active layers may threaten the safety of pile foundation in permafrost. It can cause a large uplift force, which contributes to the destructive movement of pile foundation (Andersland and Ladanyi, 2003). Additionally, the heaved pile may not return to its original position at the end of the thaw period owing to the support provided by the adfreezing bond force of the permafrost to the pile shaft. Furthermore, the uplift would be cumulated after several seasonal freeze-thaw cycles (Johnston, 1981). For a pile foundation in permafrost region, the total uplift force is a function of the unit tangential frost-heave forces (UTFF) and the area of the foundation in contact with the active layer. Therefore, to resist the uplift, the precise value of the tangential frost-heave forces (TFF) must be determined. Considering the perimeter of a pile, frost line, and minimum temperature of an active layer, Tsytovich (1959) proposed Dalmatov's equation to estimate the TFF. Subsequently, Penner and Irwin (1969) reported that Dalmatov's equation agreed well with the data acquired from field experiments. Based on the frost heaving deformation theory of foundation soil, He et al. (2015) derived an integral equation for three-dimensional viscoelastic problem of pile frost heaving force computation. Torgersen (1976) summarized the typical limiting tangential adfreezing stress values for several material types. Liu (2018) proposed a model to simulate frost jacking performances of a pile foundation, which was validated by a case study of simplified bridge pile foundation in permafrost region. Vyalov and Porkhaev (1976) recommended the design values of UTFF to be 80 kPa for the soil temperatures above −3°C and 60 kPa for those below −3°C. Liu (1993) discussed the distribution of tangential stress with the penetration of frost line. For the control measures, the screw piles were introduced to reduce frost diseases, and a series of laboratory tests and numerical simulations were conducted to evaluate the frost jacking characteristics of screw piles (Wang et al., 2017a; Wang et al., 2017b; Wang et al., 2018). A fiberglass reinforced plastic cover was proposed to relieve the frost jacking of pile foundation, and the control effect of the frost jack was assessed (Wen et al., 2016). Jiang et al. (2014) determined that two-phase closed thermosyphons can significantly restrain the frost jacking of pile foundation. Zhou et al. (2021) numerically researched the frost jacking behavior of pile foundations with and without two-phase closed thermosyphons in permafrost regions. Few studies have reported the TFF of cast-in-place pile foundation, particularly in permafrost regions. Because many variables are involved and that the material type and surface condition are key factors that govern the TFF, the existing research results barely serve as guides for the design of cast-in-place pile foundation. Hence, it is necessary to conduct field studies to determine the TFF magnitude of cast-in-place pile foundation.

Generally, the thermal regime of cast-in-place pile foundation buried in permafrost during the construction period has been the primary foci of research to date. However, the thermal and mechanical characteristics of pile foundation during operation are less well understood. The purposes of this study are primarily to:

1) Investigate the characteristics of the thermal regime of cast-in-place pile foundation during the operation period;
2) Evaluate the tangential frost-heave forces of cast-in-place pile foundation.

Hence, a field experiment was conducted on a site along the China National Highway 214 (G214) in a permafrost region of the Qinghai–Tibet plateau. Based on monitored data, we analyzed the effect of the cast-in-place pile foundation on the thermal regime and predicted the magnitude of TFF. The results will provide essential references for the structure design and stability maintenance of cast-in-place pile foundation in permafrost regions.

EXPERIMENTAL SITE AND MONITORING STUDIES

The experimental site was located in the Huashixia Area of Maduo County, Qinghai Province, Western China (**Figure 1A**). The elevation was approximately 4,300 m, and the permafrost table was approximately 2.5 m deep. An ice-rich frozen layer existed near the permafrost table. The mean annual ground temperature was about −0.7°C, signifying a region of unstable warm permafrost (Ma et al., 2008), which was highly sensitive to climate change. More precisely, permafrost degradation would more easily weaken the freezing strength and anchorage capacity of pile foundations in this area. Thus, it is representative to conduct the study on thermal regime and frost jacking of pile foundation in this experimental site.

The soil around the piles can be divided into three layers: silty clay (0–2 m), sand with gravel (2–8 m), and weathered mudstone (below 8 m). Two pile foundations, of diameter 1.2 m, were cast with C30 concrete (mixed with silicate cement) on the site in October 2012, and their lengths were 20 and 30 m. The main reinforcement in each pile foundation consisted of 28 ribbed reinforced bars with the diameter of 22 mm. A load exceeding 120 t was applied on each pile foundation on 4 November 2015.

Thermistors were instrumented along the pile sides and fixed on the reinforcement cages, as shown in **Figure 1B**. A borehole more than 10 m from the piles was drilled, and the thermistors were fixed in it to examine the natural ground temperature. Rebar stress gauges were installed in the reinforcement cage, and a protective layer of thickness approximately 7 cm existed between the reinforcement cage and the pile foundation surface. The depths of the monitoring points are summarized in **Table 1** and **Table 2**. Data were collected using data loggers at 2:00, 8:00, 14:00, and 20:00.

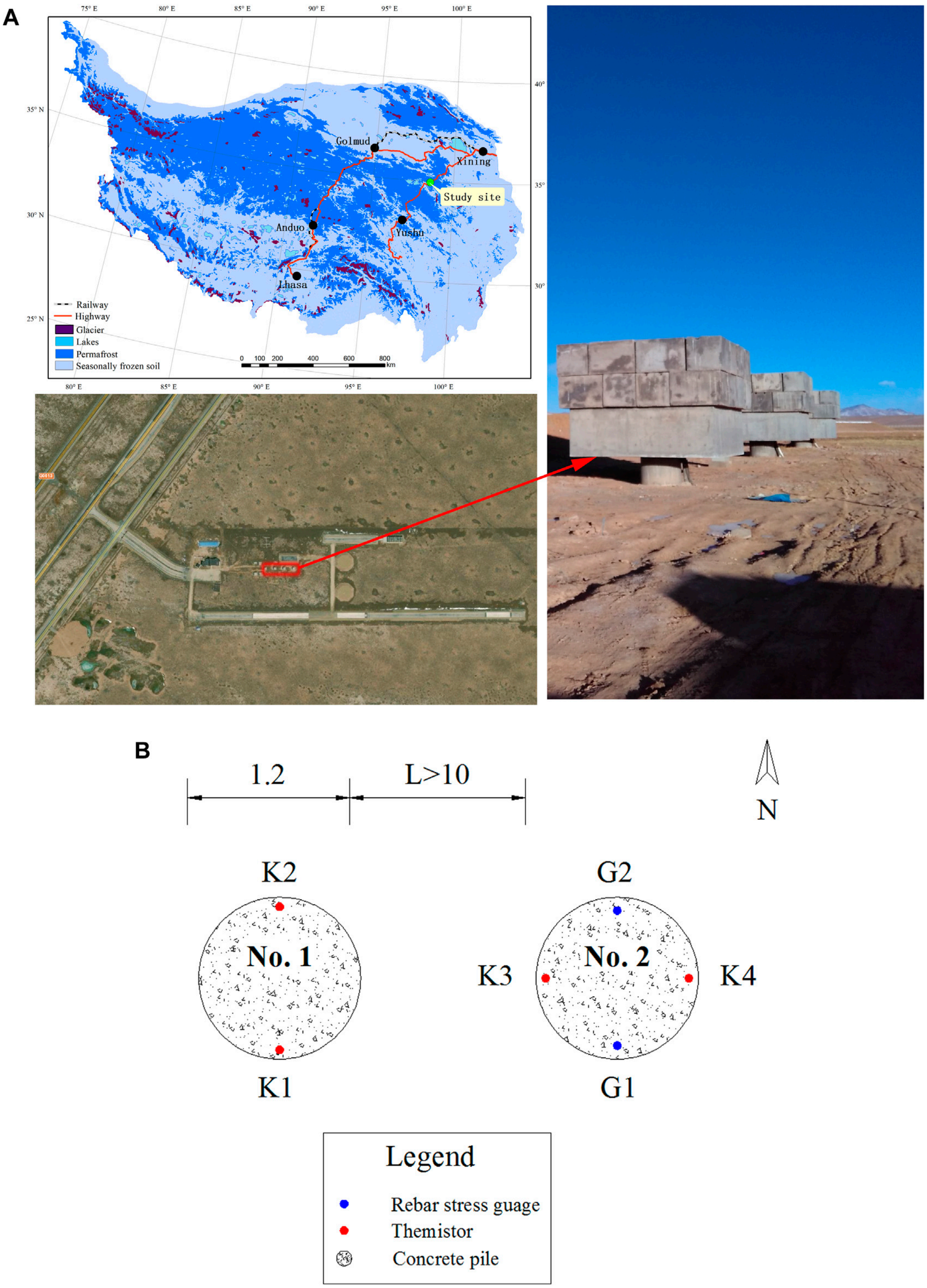

FIGURE 1 | Experimental site.

TABLE 1 | Depths of the thermistors.

	Borehole	Depths (m)
Natural ground	Natural borehole	0, −0.5, −1, −1.5, −2, −2.5, −3, −3.5, −4, −4.5, −5, −6, −7, −8, −9, −10
No. 1	K 1, K 2	0, −0.5, −1, −1.5, −2, −2.5, −3, −3.5, −4, −4.5, −5, −5.5, −6, −6.5, −7, 7.5, −8, −8.5, −9, −9.5, −10,−11, −12, −13, −14, −15, −16, −17, −18, −19, −20
No. 2	K 3, K 4	0, −0.5, −1, −1.5, −2, −2.5, −3, −3.5, −4, −4.5, −5, −5.5, −6, −6.5, −7, 7.5, −8, −8.5, −9, −9.5, −10, −11, −12, −13, −14, −15, −16, −17, −18, −19, −20, −21, −22, −23, −24, −25, −26, −27, −28, −29, −30

TABLE 2 | Depths of the rebar stress gauges.

	Borehole	Depths (m)
No. 2	G 1	−5.2, −10.7, −11.8, −12.9, −16.2, −17.3, −18.4, −21.6, −25.8
	G 2	−5.2, −6.3, −7.4, −9.6, −11.8, −14, −16.2, −17.3, −18.4, −19.5, −21.6, −23.7, −27.9, −30

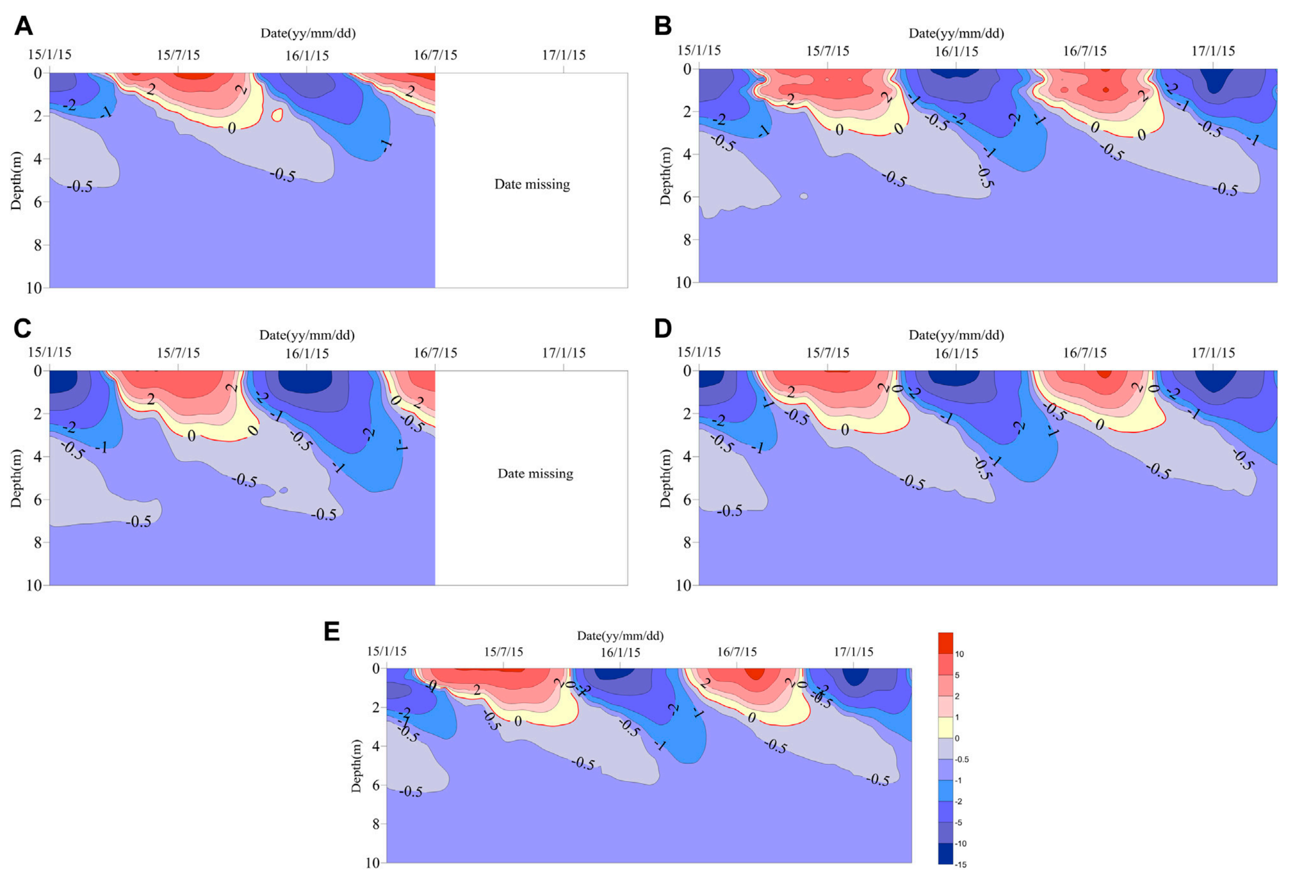

FIGURE 2 | Freeze-thaw process of the boreholes.

RESULTS AND ANALYSIS

Thermal Characteristic of the Pile Foundation

To investigate the effect of the pile foundation, **Figure 2** is presented to depict the freeze-thaw process of the natural ground and pile sides. Little difference between the two cycles in the isotherms of 0 and -0.5°C can be seen in **Figures 2B,D,E**. This phenomenon illustrated the pile foundations had completed the freezeback. As shown, a visible distinction existed between the natural ground and pile sides in the freeze-thaw process. First, the natural permafrost table was at the depth of 2.6 m in 2015

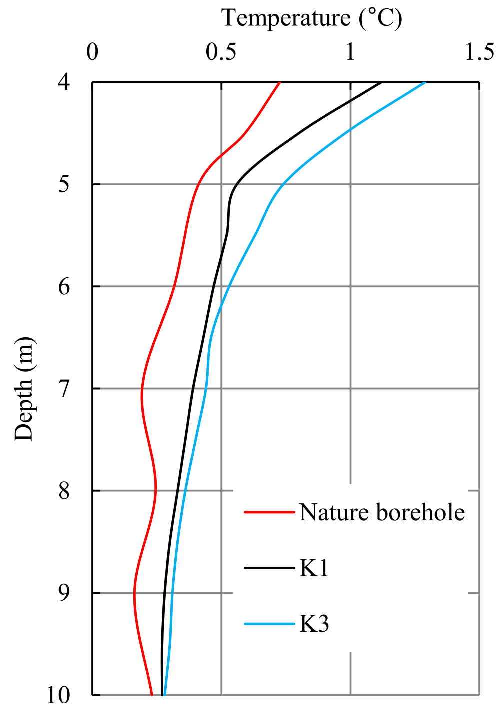

FIGURE 3 | Annual range of ground temperature of pile sides and natural borehole.

(**Figure 2A**); however, for the pile side, it ranged from three to 3.3 m (**Figure 2B–E**). Next, the −0.5°C isotherm of the natural borehole could reach the depth of 5.1 m in March 2016, which was 0.9–1.7 m shallower than that of the boreholes along the pile sides. Subsequently, the area encircled by the −1°C isotherm in the natural borehole was significantly smaller than that in boreholes K1, K2, and K3. The thermal conductivity and thermal capacity of the pile foundation were 2.94 W/(m•°C) and 2,449 kJ/(m3•°C), respectively (National Standards of the People's Republic of China, 2016). The freeze-thaw process of the surrounding soil was significantly affected by the pile foundation. This attributed to the thermal conductivity of the pile, which enhanced the heat transfer between the soil and atmosphere. As shown in **Figure 2B,C** little difference can be seen between the depths of their permafrost tables. This characteristic was also observed on the east and west sides of pile No. 2 (**Figure 2D,E**).

To quantify the effect of the concrete foundation, **Figure 3** shows the annual range of ground temperature (ARGT) along the pile sides and the nature borehole under the depth of 4 m. As shown, the ARGTs of the pile sides were significantly larger than that of the natural borehole. At the depth of 7 m, the ARGTs of boreholes K1 and K3 were more than double that of the natural borehole. Hence, the pile foundation increased the ARGT to a large degree.

The thermal regime difference between the natural ground and pile foundation demonstrated that the pile foundation acted as a heat source for the surrounding soil in warm seasons, and that the soil absorbed more heat through it. However, in the winter, the pile played a role in cooling the ground and pumped heat out of the surrounding soil. In this way, the pile foundation altered the freeze-thaw process.

Table 3 lists the time consumed by the shallow layers (0–3 m) of the boreholes to cool to the target temperatures, and the target temperatures included 0°C and −0.5°C. It is noteworthy that, to cool the active layer below 0°C, the natural borehole consumed 14.25 d, which was approximately double those consumed by boreholes K2 and K3. In addition, before the shallow layer (0–3 m) cooled to below −0.5°C, the cooling rate of the boreholes along the pile sides was more than 1.5 times that of the natural ground. The pile foundation accelerated the freeze rate of the shallow layers and reduced the cooling time significantly, which may alter the frost-heave capacity of the surrounding soil (Xu et al., 2001).

Response of Rebar Axis Force in Pile Foundation to Applied Load and Frost Heaving

Figure 4 shows the variation in rebar axis force (RAF) of pile No. 2 under the loads and the frost heaving. The vertical coordinate F, monitored using rebar stress gauges, did not represent the RAF, and its variation signified the increase or decrease in the RAF. The variation values of the RAF at several depths are listed in **Table 4**. The negative values signified compression, whereas the positive tension. A step decrease occurred 36 h after load application, and the F values of all depths changed in the same manner. Additionally, the absolute value of the variation decreased with depth in the range from 6.3 to 27.9 m. The variation value at the depth of 6.3 m was more than 11 times that at the depth of 27.9 m, indicating that the adfreezing bond force in the deep layer burdened a small percentage of the applied load. In addition, the absolute value of the F variation was larger at the depth of 6.3 m than 5.2 m; this may illustrate that the weight of the pile section exceeded the adfreezing bond force between the two depths.

Subsequently, the RAF increased sharply as the cold season was approaching, which related to the frost heaving of the surrounding active layer. From the variation values (**Table 4**) and ratio (**Figure 5**), it can be seen that the strain, caused by frost heaving, decreased with the depth. Additionally, the adfreezing bond force in the layer between 6 and 10 m alleviated most of the TFF.

To further understand the development process of the TFF, **Figure 6** is presented to show the relationship between the freeze-thaw process and the RAF variation of pile No. 2. Note that the value of F almost had not increased until the 0°C isotherm disappeared. Subsequently, it increased with the thickness decrease of the soil layer above −0.5°C. Furthermore, the F values reached the maximum on March 29, 2016 when the −0.5°C isotherm disappeared. The thickness of the frost heaving layer was approximately double

TABLE 3 | Time consumed by shallow layers (0–3 m) to cool to below 0 °C and −0.5°C during freezing period in late 2015.

Target temperature (°C)	Cooling time (d)			
	Nature borehole	K 1	K 2	K 3
0	14.25	8	7.25	7.25
−0.5	148.83	90.00	89.75	93.00

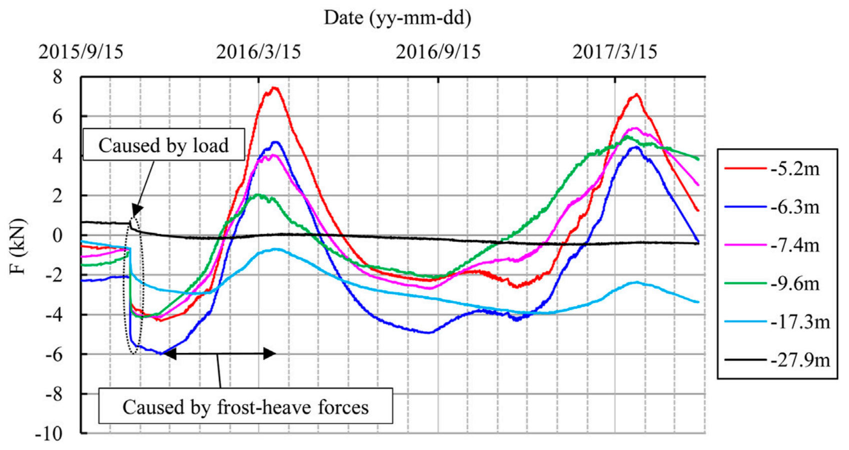

FIGURE 4 | Variations of rebar axis force at different depths of pile No. 2.

TABLE 4 | Variations of rebar axis force caused by load and TFF.

Depth (m)	The variations caused by the load in 35 h (kN)	The variations caused by the TFF (kN)
−5.2	−2.72	11.78
−6.3	−3.18	10.72
−7.4	−3.09	8.19
−9.6	−2.97	6.22
−17.3	−1.21	2.53
−27.9	−0.28	0.83

that of the active layer. This phenomenon may be attributed to the existence and migration of unfrozen water within the soil (Qiu et al., 1994). In other words, the soil first contained both ice and unfrozen water when the temperature dropped below 0°C. The unfrozen water was subjected to the exist temperature gradient, and moved toward the colder direction. It enhanced the ice lens formation and frost heaving. The maximum uplift force occurred when the ground was completely saturated with ice (and little unfrozen water). After that, the heaving almost stopped development. Not only the active layer, but also the permafrost with unfrozen water can cause the TFF in the freezing process.

It is noteworthy that all the F magnitudes under frost heaving were significantly higher than those before load application (**Figure 5**). And the force diagram of shallow pile section is shown in **Figure 7**. Meanwhile, the relationship between the tangential frost-heave forces [$Q(z)$], applied load (P) and axial force of pile shaft at the depth of 6.3 m [N (6.3)] can be described as **Eq. 1**:

$$Q(z) = \pi D \int_0^{6.3} q(z)\mathrm{d}z = P + N(6.3) \tag{1}$$

Where D is the diameter of pile, $q(z)$ is the unit tangential frost-heave forces and the z is the depth.

It can be concluded that the maximum TFF was more than the load (120 t). According to above scenario, the TFF was generated

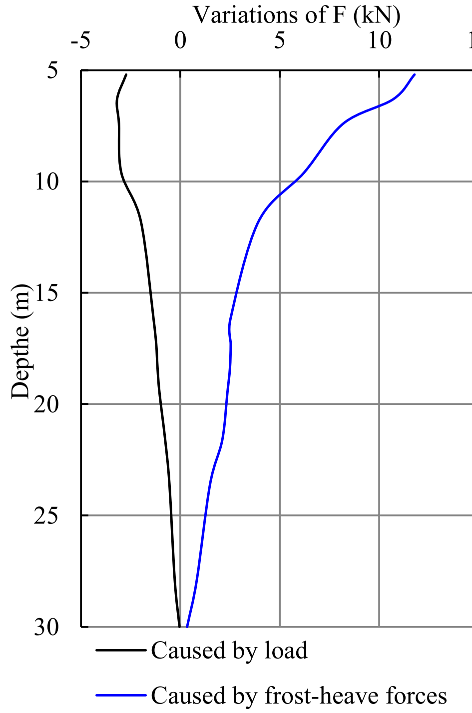

FIGURE 5 | Variations of RAF with depth.

by the frost heaving layer, and its thickness was approximately 6 m. Combining with the load magnitude and the pile diameter, the maximum UTFF should exceed 52.04 kPa.

Distribution of Adfreezing Force Along Pile Under Applied Load and Frost Heaving

Figure 8 shows the force diagram of pile. According to the existing literature (Weaver and Morgenstern, 1981; Tang et al.,

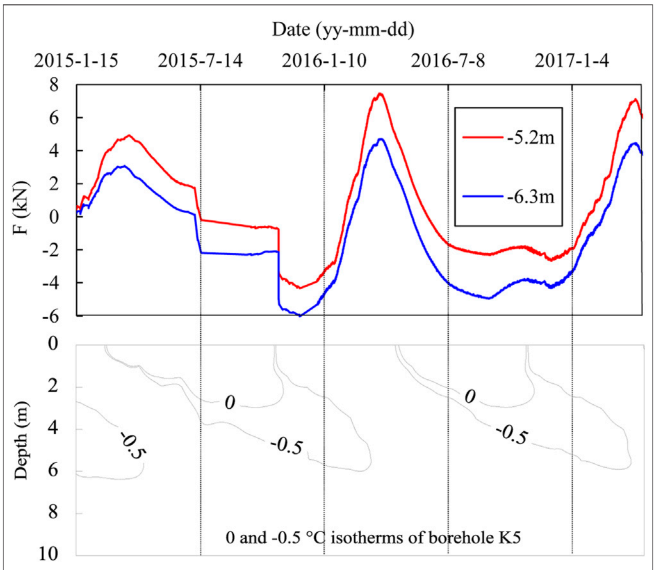

FIGURE 6 | Time series of the freeze-thaw process and seasonal variations of RAFs at depths of –5.2 and –6.3 m of pile No. 2.

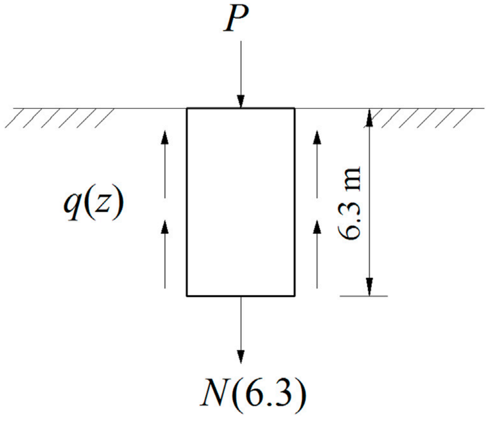

FIGURE 7 | Force diagram of pile section under frost heaving.

2019; Wang et al., 2021), the corresponding profiles of axial force were calculated from strains multiplied by the pile axial rigidity, and can be described as:

$$N = E \cdot A \cdot \varepsilon \tag{2}$$

Where E is the Young's modulus of the pile, and A is the cross-section area.

The shaft resistance can be described as:

$$q(z,t) = \frac{-1}{\pi D} \cdot \frac{\partial N(z,t)}{\partial z} \tag{3}$$

Where t is the time.

The shaft resistance of the *k-th* soil layer were calculated using axial force at each soil layer, based on **Eq. 4**:

$$q_k = \frac{-1}{\pi D} \cdot \frac{N_{k+1} - N_k}{l_k} \tag{4}$$

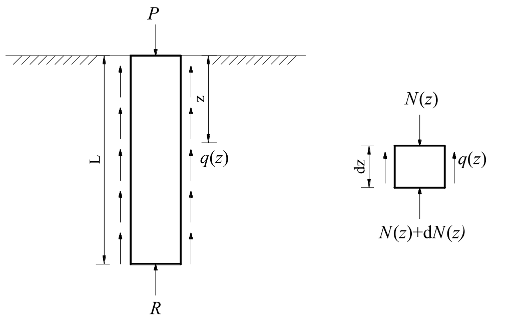

FIGURE 8 | Force diagram of pile **(A)** Variations of RAF with depth **(B)** Distribution of temperature with depth.

Where N_{k+1} and N_k are the axial forces of pile shaft at the bottom and top of the *k-th* soil layer; l_k is the thickness of the *k-th* soil layer.

The Young's modulus of the piles is estimated using **Eq. 5**:

$$E = \frac{(E_c A_c + E_a A_a)}{A} \tag{5}$$

Where E_c and E_a are the Young's modulus of concrete and steel rebar, respectively; A_c, A_a, and A are the cross-sectional areas of concrete, rebars, and pile, respectively.

The relationship between strains of steel rebar and pile can be described as **Eq. 6**, **Eq. 7**, and **Eq. 8**:

$$\varepsilon(z,t) = \varepsilon_a(z,t) \tag{6}$$

$$\frac{N(z,t)}{EA} = \frac{N_a(z,t)}{E_a A_a} \tag{7}$$

$$\frac{\frac{\partial N(z)}{\partial t}}{EA} = \frac{\frac{\partial N_a(z)}{\partial t}}{E_a A_a} \tag{8}$$

To illustrate the response of rebar axial force to the applied load, according to the measured results, **Figure 9** shows the variations of RAF and temperature with depth after load application. It can be seen that the pile side temperature have dropped below 0°C when the load was applied on the pile (**Figure 9B**). The pile shaft experienced a significant compression processes in the initial period (**Figure 9A**). The compression development tendency attenuated, and got into a relatively stable state a month later. The distribution characteristics of variable quantity of the RAF along the pile side were similar at the different times. It should be noted that the compression faded with the depth due to the effect of adfreezing bond force of the permafrost to the pile shaft.

In order to further explain the interaction of the pile-soil interface in an intuitive way, the coefficient $\alpha(z) = \Delta N_a(z)/\Delta N_a(6.3)$ was selected as an index to assess the strain distribution of pile under the depth of 6.3 m according to **Eq. 8**. **Table 5** lists the $\alpha(z)$ with the depth at different times. It can be found that the α under the depth of 18.4 m gradually increase with time in a month after load application, indicating that the deeper pile section needed a considerable period to response to the applied load. Meanwhile, the α (30) range from 1.29% to 5.72% during this

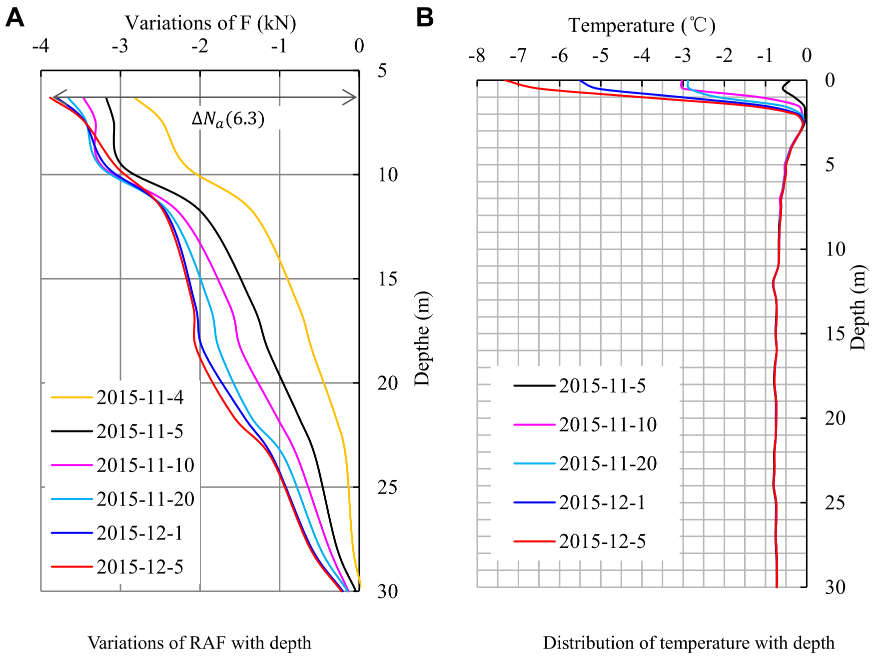

FIGURE 9 | Variations of RAF and temperature with depth after load application **(A)** Variations of RAF with depth **(B)** Distribution of temperature with depth.

TABLE 5 | The coefficient α with depth at different time after load application.

Depths (m)	$\Delta N_a(z)/\Delta N_a(6.3)$ (%)									
	6.3	**7.4**	**9.6**	**11.8**	**16.2**	**18.4**	**21.6**	**23.6**	**27.9**	**30**
2015-11-5	100.00	97.06	93.37	62.32	42.25	36.00	23.97	17.21	8.84	1.29
2015-11-10	100.00	95.70	93.20	65.48	47.18	42.80	29.99	22.28	10.97	3.86
2015-11-20	100.00	93.95	88.92	65.33	51.51	48.05	37.23	25.62	13.51	3.93
2015-12-1	100.00	91.02	83.64	64.02	54.34	51.65	38.21	28.50	15.87	5.40
2015-12-5	100.00	89.19	78.65	63.14	53.87	52.54	40.70	28.40	16.01	5.72

period. In other words, the end-bearing resistance only burdened less than 5.72% of applied load, which was consistent with that reported in Aksenov and Kistanov (2008), Johnston (1981) and Andersland and Ladanyi (2003).

The relationship between the end-bearing resistance and shaft resistance can be described by **Eq. 9**:

$$R = P - \pi D \int_0^L q(z)\mathrm{d}z \tag{9}$$

Thus, the α can also reflect the effect of shaft resistance on the pile axial force. The maximum shaft resistance appeared in the layer 9.6–11.8 m on November 5, 2015, which was approximately 3.9 times that between the depths of 27.9 and 30 m. Furthermore, the shaft resistance took more than 94.28% of the applied load, which was a significant specificity comparing with the pile in unfrozen soil. The shaft resistance was mainly provided by freezing strength of permafrost to the concrete pile, which owned a significant characteristic of temperature-dependent. Thus, a frozen state for the surrounding soil is the key factor that guarantees the stability of pile foundation in permafrost regions. Further investigations on controlling the thermal regime of pile foundation in permafrost are necessary for the operation safety of superstructure.

It can be confirmed that the frost action of active layer subjected a considerably large uplift forces to the pile foundation (**Figure 4**). To explore the effect of frost heaving on the pile foundation, **Figure 10** presents the variations of RAF and temperature with depth during freezing period. A part of pile shaft was stretched under the frost action of active layer on January 25, 2017. Then, this tension of pile shaft further developed as the freezing front saturated downward. Until April 5, 2017, the tension had occurred on the pile section above a depth of 21.6 m, when the uplift forces should reach the maximum. It can be concluded that the influence depth of frost action on the pile foundation may reach a depth of 21.6 m. In other words, the adfreezing bond force of the layer between 6.3 and 21.6 m played a major role in anchoring the pile, which overcame most of adfreezing uplift forces caused by the frost action of shallow layer.

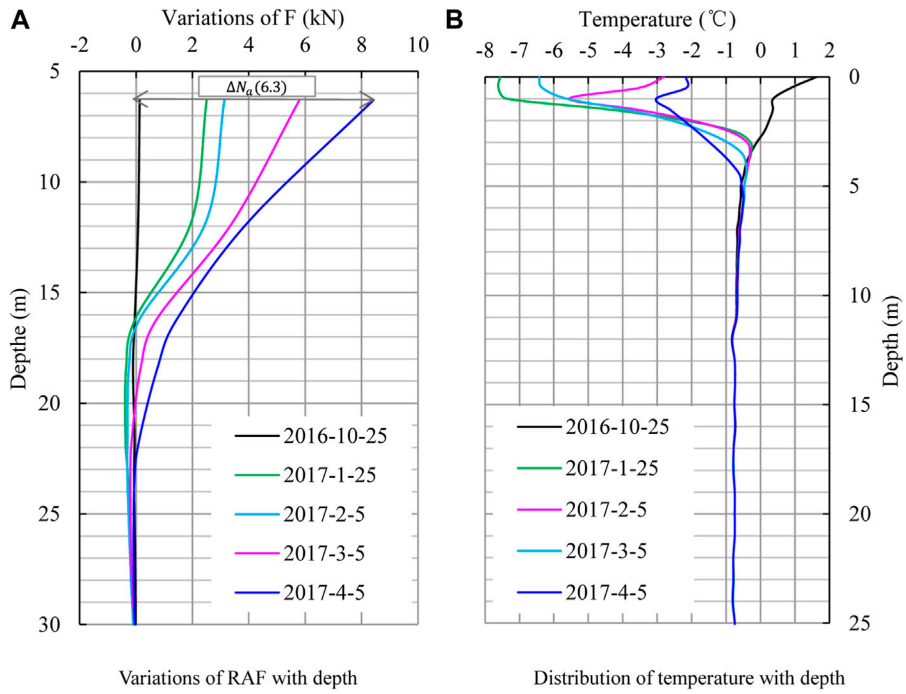

FIGURE 10 | Variations of RAF and pile side temperature with depth during freezing period.

TABLE 6 | The coefficient α with depth at different time under adfreezing uplift forces.

Depths(m)	$\Delta N_a(z)/\Delta N_a(6.3)$ (%)							
	6.3	11.8	16.2	18.4	21.6	23.6	27.9	30
2016-10-25	100.00	59.87						
2017-1-25	100.00	78.31						
2017-2-5	100.00	79.14	4.09			Compression		
2017-3-5	100.00	59.31	12.68	2.84				
2017-4-5	100.00	47.32	17.22	9.04	1.46			

For further exploring the distribution of shaft resistance of permafrost to the pile shaft, **Table 6** lists the coefficient α with depth at different time under adfreezing uplift forces. The thickness of the frost heaving layer was approximately 6 m in view of the above-mentioned facts. The total shaft resistance of the first (6.3–11.8 m) layer overcame approximately 52.68% of the adfreezing uplift forces on April 5, 2017. The unit adfreezing force of this layer was approximately 4.04 times that of the 4th (18.4–21.6 m) layer.

CONCLUSION

A field experiment was conducted in this study. Based on the monitoring data, we discussed the effect of cast-in-place pile foundation on the geotemperature during operation, and quantitatively analyzed the TFF. Based on the results, the following conclusions were obtained:

1) The cast-in-place pile foundation acted as a better thermal conductor in the ground and enhanced the heat exchange between the atmosphere and soil. Furthermore, it increased the annual range of the surrounding ground temperature.
2) The pile foundation increased the permafrost table depth by 0.4–0.7 m in contrast to natural ground, which accounted for 0.33–0.58 times the pile diameter. It should be an important consideration in the stability maintenance of pile foundation during operation.
3) The TFF increased significantly when the soil temperature dropped from 0 to −0.5°C. The thickness of the frost heaving layer was approximately double that of the active layer, and the maximum UTFF should be beyond 52.04 kPa. This lesson will serve as a guide for the design of cast-in-place pile foundation.
4) More than 94.28% of the bearing capacity was contributed by freezing strength for cast-in-place pile foundation in permafrost regions. The adfreezing bond force of

permafrost to pile shaft played an important role in burdening applied load and resisting the frost jacking.

In this study, it was discovered that the cast-in-place pile foundation may negatively affect the stability in the thermal regime. In future experiments, we will propose measures to mitigate this effect. In addition, the soil type and the characteristics of pile structure are two key factors that govern the TFF; therefore, we will discuss the influencing mechanism of the two factors in future publications.

DATA AVAILABILITY STATEMENT

The raw data supporting the conclusion of this article will be made available by the authors, without undue reservation.

AUTHOR CONTRIBUTIONS

YS: Roles/Writing—original draft, Data curation, Formal analysis, Resources, Methodology. FN: Funding acquisition, Writing—review and editing, Supervision. JF: Resources. LW: Visualization.

FUNDING

This work was supported by the Second Tibetan Plateau Scientific Expedition and Research (STEP) program (Grant No. 2019QZKK0905), the State Key Program of National Natural Science of China (Grant Nos. 42001063 and 41961011), the Program of the State Key Laboratory of Frozen Soil Engineering (Grant No. SKLFSE-ZT-202120).

REFERENCES

Aksenov, V. I., and Kistanov, O. G. (2008). Estimation of Resistance Components to an Axial Load on Piles Embedded in Permafrost. *Soil Mech. Found. Eng.* 45 (2), 71–75. doi:10.1007/s11204-008-9001-4

Andersland, O. B., and Ladanyi, B. (2003). *Frozen Ground Engineering*. Hoboken: John Wiley & Sons.

Goncharov, Y. M. (1965). Formation of the Supporting Zone Round a Pile Driven into Thawed Permafrost Ground. *Soil Mech. Found. Eng.* (2), 11–14. doi:10.1007/bf01704772

He, F., Wang, X., Jiang, D. J., Liang, Q. G., and Ren, M. Y. (2015). Research on Three-Dimensional Viscoelastic Frost Heaving Force Problem of Pile Foundation. *Rock Soil Mech.* 36 (9), 2510–2516. doi:10.16285/j.rsm.2015.09.010

Jia, X. Y., Yang, Y. Q., and Li, W. J. (2004). Study of Ground Temperature Field during Pile Foundation Construction in Permafrost Regions. *Rock Soil Mech.* 25 (7), 1139–1142. doi:10.16285/j.rsm.2004.07.029

Jiang, D. J., Wang, X., Liu, D. R., and Xia, Q. (2014). Experimental Study of Stability of Piled Foundation with Thermosyphons of Power Transmission tower along Qinghai—Tibet Railway in Permafrost Regions. *Chin. J. Rock Mech. Eng.* 33 (2), 4258–4263. doi:10.13722/j.cnki.jrme.2014.s2.108

Johnston, G. H. (1981). *Permafrost Engineering Design and Construction*. Hoboken: John Wiley & Sons. Available at: https://kns.cnki.net/kcms/detail/detail.aspx?dbcode=CJFDanddbname=CJFD2005andfilename=BFJT200501003anduniplatform=NZKPTandv=7Dj9mr7fKjNluVA12twfXLfyc5485JVNv7Zrxabnsc4BvoKVkm5VAHM50zFc_sVj

Li, X. H., Yang, Y. P., and Wei, Q. C. (2005). Numerical Simulation of Pile Foundation Conduction at Different Molding Temperature in Permafrost Regions. *J. Beijing Jiaotong Univ.* 29 (1), 10–13.

Liu, H. X. (1993). Discussion on the Distribution of Tangential Frost Heaving Forces along the Lateral Surface of Pile. *J. Glaciol. Geocryol.* 15 (2), 289–292. Available at: https://kns.cnki.net/kcms/detail/detail.aspx?dbcode=CJFDanddbname=CJFD9093andfilename=BCDT199302015anduniplatform=NZKPTandv=H7SBZ8HowYIOv4PpLyfRUaCslsu8-UPF57elX6zPKcGOvnB-4e9olvSWXB_y9RdP

Liu, J., Wang, T., Tai, B., and Lv, P. (2020). A Method for Frost Jacking Prediction of Single Pile in Permafrost. *Acta Geotech.* 15, 455–470. doi:10.1007/s11440-018-0711-0

Ma, W., Feng, G., Wu, Q., and Wu, J. (2008). Analyses of Temperature fields under the Embankment with Crushed-Rock Structures along the Qinghai-Tibet Railway. *Cold Regions Sci. Tech.* 53 (3), 259–270. doi:10.1016/j.coldregions.2007.08.001

Ma, W., and Wang, D. Y. (2014). *Frozen Soil Mechanics*. Beijing: Science Press.

National Standards of the People's Republic of China (2016). *GB 50010-2016 Code for Design of concrete Structures*. Beijing: China Architecture & Building Press.

Penner, E., and Irwin, W. W. (1969). Adfreezing of Leda clay to Anchored Footing Columns. *Can. Geotech. J.* 6 (3), 327–337. doi:10.1139/t69-031

Qiu, G. Q., Liu, J. R., and Liu, H. X. (1994). *Geocryological Glossary*. Lanzhou: Gansu Science and Technology Press.

S. S. Vyalov and G. V. Porkhaev (Editors) (1976). *Handbook for the Design of Bases and Foundations of Building and Other Structures on Permafrost* (Ottawa: Nat. Res. Counc. Can, Tech. Transl. TT), 1865.

Tang, L., Wang, K., Deng, L., Yang, G., Chen, J., and Jin, L. (2019). Axial Loading Behaviour of Laboratory concrete Piles Subjected to Permafrost Degradation. *Cold Regions Sci. Tech.* 166, 102820. doi:10.1016/j.coldregions.2019.102820

Tang, L. Y., and Yang, G. X. (2010). Thermal Effects of Pile Construction on Pile Foundation in Permafrost Regions. *Chin. J. Geotech. Eng.* 32 (9), 1350–1353. Available at: https://kns.cnki.net/kcms/detail/detail.aspx?dbcode=CJFDanddbname=CJFD2010andfilename=YTGC201009009anduniplatform=NZKPTandv=H8NGq_iBN1VQS-dbIP4ZF0ysLl3-pmUsVqkoEdjRuIcxEISGOY21RqMkUrwUGkVS

Torgersen, S. E. (1976). Frost protection with Open Foundations (In Norwegian). *Frost i Jord* 17 (10), 367–373.

Tsytovich, N. A. (1959). *Principles of Geocryology, Part 2, Chap. 3*, 1239. Ottawa: Nat. Res. Counc. Can, Tech. Transl. TT.

Wang, J., Zhu, H.-H., Mei, G.-X., Xiao, T., and Liu, Z.-Y. (2021). Field Monitoring of Bearing Capacity Efficiency of Permeable Pipe Pile in Clayey Soil: A Comparative Study. *Measurement* 186, 110151. doi:10.1016/j.measurement.2021.110151

Wang, T. F., Liu, J. K., Tai, B. W., and ZangLv, P. (2018). Model Tests on Frost Jacking Behaviors of Helical Steel Piles. *Chin. J. Rock Mech. Eng.* 40 (6), 1084–1092. Available at: https://kns.cnki.net/KXReader/Detail?invoice=Ch1%2B6hbk4FUt%2F36dRyx9Tv4aetDPtys1JZVGRwSmBWZ1qYz1wstxOgNXRMBkU8iWVGrOkYDTcSsh1H%2BXbG90sxXKO%2F6B68TyFtt3ChUumAhvLIJWQUNT%2FDhauOTedynbeVlw4CGrHbuxM7B%2BghFhBiKeRW8uGV9YSumpRehkwso%3DandDBCODE=CJFDandFileName=YTGC201806017andTABLEName=cjfdlast2018andnonce=ED75EB94C603454883711AA9EFEA4C29anduid=andTIMESTAMP=1643104086714

Wang, T., Liu, J., Tai, B., Zang, C., and Zhang, Z. (2017b). Frost Jacking Characteristics of Screw Piles in Seasonally Frozen Regions Based on Thermo-Mechanical Simulations. *Comput. Geotechnics* 91, 27–38. doi:10.1016/j.compgeo.2017.06.018

Wang, T., Liu, J., Tian, Y., and Lv, P. (2017a). Frost Jacking Characteristics of Screw Piles by Model Testing. *Cold Regions Sci. Tech.* 138, 98–107. doi:10.1016/j.coldregions.2017.03.008

Wang, X., Jiang, D. J., Liu, D. R., and He, F. (2013). Experimental Study of Bearing Characteristics of Large-Diameter Cast-In-Place Bored Pile under Non-refreezing Condition in Low-Temperature Permafrost Ground. *Chinj. Rock Mech. Eng.* 32 (9), 1807–1812. Available at: https://kns.cnki.net/kcms/detail/detail.aspx?dbcode=CJFDanddbname=CJFD2013andfilename=YSLX201309012anduniplatform=NZKPTandv=Dn4xAiK4szqoyMMq4G-4O8AdO4FY4LnBmVcb2hk2yeesaBZ7zeIiWyl7ncmD0WMh

Wang, X., Jiang, D. J., Zhao, X. Y., and Liu, D. R. (2005). Experimental Study on Bearing Features of Bored Pile under Non-refreezing Condition in Permafrost Region. *Chin. J. Geotech. Eng.* 27 (1), 81–84.

Wang, X., Jiang, D. J., Zhao, X. Y., Shi, C. S., and Wang, C. H. (2004). An Experimental Study on Refreezing Characteristics of Large-Diameter Bored Pile in Different Permafrost Areas of the Qinghai-Tibet Plateau. *Chin. J. Rock Mech. Eng.* 23 (24), 4206–4211.

Weaver, J. S., and Morgenstern, N. R. (1981). Pile Design in Permafrost. *Can. Geotech. J.* 18 (3), 357–370. doi:10.1139/t81-043

Wen, Z., Yu, Q., Ma, W., Dong, S., Wang, D., Niu, F., et al. (2016). Experimental Investigation on the Effect of Fiberglass Reinforced Plastic Cover on Adfreeze Bond Strength. *Cold Regions Sci. Tech.* 131, 108–115. doi:10.1016/j.coldregions.2016.07.009

Wu, Y. P., Guo, C. X., Zhao, S. Y., Zhang, L. X., and Zhu, Y. L. (2004). Influence of Casting Temperature of Single Pile on Temperature Field of Ground in Permafrost of Qinghai-Tibet Plateau. *J. China Railw. Soc.* 6, 81–85.

Wu, Y. P., Su, Q., Guo, C. X., Zhu, Y. L., Zhang, L. X., and Zhao, S. Y. (2006). Nonlinear Analysis of Ground Refreezing Process for Pile Group Bridge Foundation in Permafrost. *China Civ. Eng. J.* 39 (2), 78–84.

Xu, X. Z., Wang, J. C., and Zhang, L. X. (2001). *Frozen Soil Physics*. Beijing: Science Press.

Yuan, X. Z., Ma, W., and Liu, Y. Z. (2005). Study on thermal Regime of High-Temperature Frozen Soil while Construction of Cast-In-Place Pile. *Chin. J. Rock Mech. Eng.* 6, 1052–1055.

Zhang, J. Z., Zhou, Y. J., and Zhou, G. (2010). Study on the Freezing-Back Time of Bridge Pile Foundation in the Permafrost Regions of Qinghai-Tibet Highway. *Highway* 1, 33–38.

Zhou, Y., Wang, X., Niu, F., He, F., Guo, C., Liu, D., et al. (2021). Frost Jacking Characteristics of Transmission Tower Pile Foundations with and without Thermosyphons in Permafrost Regions of Qinghai-Tibet Plateau. *J. Cold Reg. Eng.* 35 (2), 04021004. doi:10.1061/(asce)cr.1943-5495.0000246

Conflict of Interest: The authors declare that the research was conducted in the absence of any commercial or financial relationships that could be construed as a potential conflict of interest.

Publisher's Note: All claims expressed in this article are solely those of the authors and do not necessarily represent those of their affiliated organizations, or those of the publisher, the editors and the reviewers. Any product that may be evaluated in this article, or claim that may be made by its manufacturer, is not guaranteed or endorsed by the publisher.